Physica B 175 (1991) 81–86
North-Holland

Photonic band structure: Non-spherical atoms in the face-centered-cubic case

E. Yablonovitch
Bell Communications Research, Navesink Research Center, Red Bank, NJ 07701-7040, USA

K.M. Leung
Dept. of Physics, Polytechnic University, Brooklyn, NY 11201, USA

We introduce a practical, new, face-centered-cubic (FCC) dielectric structure which simultaneously solves two of the outstanding problems in photonic band structure. In this new "photonic crystal" the atoms are non-spherical, lifting the degeneracy at the W-point of the Brillouin zone, and permitting a full photonic band gap rather than a pseudogap. Furthermore, this fully 3-dimensional FCC structure lends itself readily to microfabrication on the scale of optical wavelengths. It is created by simply drilling 3 sets of holes 35.26° off the vertical into the top surface of a solid slab or wafer, as can be done for example by chemical beam assisted ion etching. It appears that the application of photonic band gaps to semiconductor physics, optical and atomic physics may soon be practical.

Among the analogies between optics and micro-electronics, one of the most compelling is that between electron waves in a crystal and photon waves in a three-dimensionally periodic dielectric structure. The behaviour of both waves should be described by band theory. The idea of photonic band structure [1, 2] is gaining rapid [3–6] acceptance. The concepts of reciprocal space, Brillouin zones, dispersion relations, Bloch wave functions, Van Hove singularities, etc., are now being applied to optical waves.

A search has been underway for three-dimensional topologies in which a "photonic band gap" can open up. This would be an energy band in which optical modes, spontaneous emission, and zero point fluctuations are all absent. Indeed, a photonic band gap would be essentially ideal since optical dielectric response can be real and dissipationless.

In addition to the obvious applications in atomic physics, inhibited spontaneous emission can now begin to play a role in semiconductor and solid state electronics. If the photonic band gap overlaps the electronic band edge, spontaneous electron–hole recombination is rigorously forbidden. In a semiconductor laser, this would lead to near unity quantum efficiency into the lasing mode. Photon number state squeezing [7] into that mode would be greatly enhanced.

There have been two main challenges in this field. The first was to show that a full 3-dimensional "photonic band gap" could actually exist in some type of dielectric structure. The second was to show that such a forbidden gap could be created in a micro-structure amenable to practical micro-fabrication.

At the outset it was realized [1] that a face-centered-cubic (FCC) array in real space would produce the "roundest" Brillouin zone in reciprocal space. Such a sphere-like Brillouin zone improves the prospects for a forbidden gap to overlap all the way around its surface. But it was unclear what should be the real-space shape of the atoms in the FCC array. The original suggestion [1] called for cubic atoms. Later, the first experimental effort [8] concentrated on dielectric spheres and on spherical voids in a dielectric background. The spherical void structure appeared to perform particularly well. The history of this field has been a search for that optimal

0921-4526/91/$03.50

3-dimensional dielectric geometry, favored by nature and by Maxwell's equations.

During this same period, electronic band theorists began calculating photonic band structure. It rapidly became apparent that the familiar scalar wave band theory, so frequently used for electrons in solids, was in utter disagreement with experiment on photons [9–12]. Recently a full vector-wave band theory [3–5] became available, which not only agreed with experiment, it high-lighted some discrepancies in experiment. Vector-wave band theory showed that spherical atomic symmetry produced a degeneracy between valence and conduction bands at the W-point of the Brillouin zone, allowing only a pseudogap, rather than a full photonic band gap. The solution to this symmetry-induced degeneracy problem is to make the atoms non-spherical.

Therefore, we introduce a practical, new, face-centered-cubic (FCC) structure which simultaneously solves two of the outstanding problems in photonic band structure: (1) In this new geometry the atoms are non-spherical, lifting the degeneracy at the W-point of the Brillouin zone, and permitting a full photonic band gap rather than a pseudogap. (2) Furthermore, this fully 3-dimensional FCC structure lends itself readily to micro-fabrication on the scale of optical wavelengths. It is created by simply drilling 3 sets of holes 35.26° off the vertical into the top surface of a solid slab or wafer, as can be done for example by reactive ion etching. At refractive index $n \approx 3.6$, typical of semiconductors, the 3-d forbidden photonic band gap width in this new structure is ~20% of its center frequency. Calculations indicate that the gap remains open for refractive indices $n \geqslant 2$.

The Wigner–Seitz (WS) unit cell of the FCC lattice is a rhombic dodecahedron as shown in fig. 1. The problem of creating an arbitrary FCC dielectric structure reduces to the problem of filling the FCC WS real-space unit-cell with an arbitrary spatial distribution of dielectric material. Real space is then filled by repeated translation and close-packing of the WS unit cells. Scientific progress in this field has been marked by improved choices of how to fill the WS unit with dielectric material. As already mentioned,

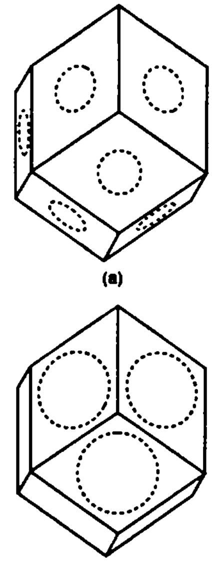

(a)

(b)

Fig. 1. The Wigner–Seitz real-space unit-cell of the FCC lattice is a rhombic dodecahedron. In ref. [8] slightly oversized spherical voids were inscribed into the unit cell, breaking through the faces, as illustrated by the dashed lines in (a). The current structure, shown in (b), is non-spherical. Cylindrical holes are drilled through the top 3 facets of the rhombic dodecahedron and exit through the bottom 3 facets. The resulting atoms are roughly cylindrical, and have a preferred axis in the vertical direction.

early proposals called for cubic [1] atoms, then spherical atoms and spherical voids [8] to be inscribed inside the WS unit cell.

Figure 1(a) shows a WS unit cell filled by an over-sized spherical void, a structure which performed rather well in ref. [8]. Since the spheres were slightly larger than close-packed, the voids broke through the surfaces of the WS unit cell as indicated by the dashed circles on the faces of the rhombic dodecahedron in fig. 1(a). In ref. [8] it was already pointed out that there was a symmetry-induced degeneracy at the W-point of the Brillouin zone in FCC structures. There was a danger that the valence and conduction bands could touch at the degeneracy, closing the photonic band gap. Based on the weight of experimental evidence however, ref. [8] argued that the degeneracy had only caused adjacent conduction band levels to touch, permitting the gap to remain open. Vector-wave band theory, which has become quite successful recently [3–5], contradicted this. It showed that the degeneracy did indeed cause valence and conduction bands to touch at W, permitting only a pseudogap rather than a full photonic band gap. Unfortunately, the finite-sized experimental sample in ref. [8] allowed inadequate resolution to detect touching at isolated points on the Brillouin zone.

The degeneracy at W can be lifted by lowering the spherical symmetry of the atoms inside the WS unit cell. We have made a close examination [13] of the degenerate wave functions at W in the nearly-free-photon model, and learned that a distortion of the spherical atoms along the ⟨1 1 1⟩-direction will lift the degeneracy. The WS unit cell in fig. 1(b) has great merit for this purpose. Holes are drilled through the top 3 facets of the rhombic dodecahedron and exit through the bottom 3 facets. The beauty of the structure in fig. 1(b) is that a stacking of WS unit cells results in straight holes which pass clear through the entire "crystal"! The "atoms" are odd-shaped, roughly cylindrical voids centered in the WS unit cell, with a preferred axis pointing to the top vertex.

An operational illustration of the construction which produces an FCC "crystal" of such WS unit cells is shown in fig. 2. A slab of material is covered by a mask containing a triangular array of holes. Three drilling operations are conducted through each hole, 35.26° off normal incidence and spread out 120° on the azimuth. The resulting criss-cross of holes below the surface of the slab produces a fully 3-dimensionally periodic FCC structure, with WS unit cells given by fig. 1(b)! The drilling can be done by a real drill bit for microwave work, or by reactive ion etching to create an FCC structure at optical wavelengths. We have fabricated such "crystals" in the microwave region by direct drilling into a commercial, low-loss, dielectric material, Emerson & Cumming Stycast-12. Its microwave refractive index, $n \sim 3.6$, is meant to correspond to that of the common semiconductors, Si, GaAs, etc. By simply scaling down the dimensions, this structure can be employed equally well at optical wavelengths. In this paper we will present the measured and calculated, ω versus k, dispersion relations for this new photonic crystal.

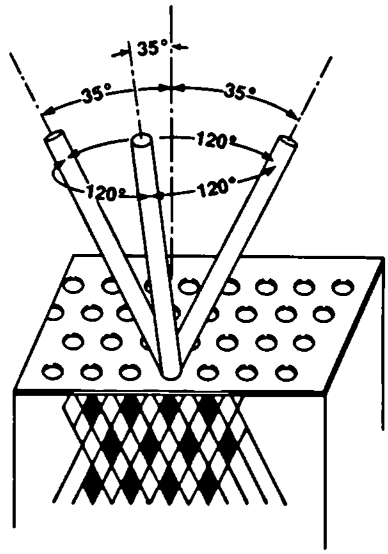

Fig. 2. The method of constructing an FCC lattice of the Wigner–Seitz cells as shown in fig. 1(b). A slab of material is covered by a mask consisting of a triangular array of holes. Each hole is drilled through 3 times, at an angle 35.26° away from normal, and spread out 120° on the azimuth. The resulting criss-cross of holes below the surface of the slab, suggested by the cross-hatching shown here, produces a fully 3-dimensionally periodic FCC structure, with unit cells as given by fig. 1(b). The drilling can be done by a real drill bit for microwave work, or by reactive ion etching to create an FCC structure at optical wavelengths.

There are other ways to break the spherical symmetry of fig. 1(a). In an important new proposal [5], Ho, Chan and Soukoulis placed two atoms in the WS unit cell, forming a diamond structure and allowing a very wide photonic band gap. Diamond symmetry can be created by supplementing the operations of fig. 2 with 3 additional drilling operations, making a total of 6 drilling directions. These 3 new drilling directions, 120° apart, would all lie within the plane of the slab. Therefore, they are somewhat difficult to implement experimentally. The 6 drilling directions correspond to the 6 inequivalent ⟨1 1 0⟩ channeling holes in the diamond structure.

We have experimentally surveyed 3 FCC structures, drilled in accordance with fig. 2, to different ratios d/a of hole diameter d to the FCC unit cube length a: $d/a = 0.361$, 0.433, and 0.469.

The removed volume fraction was approximately 62%, 70%, and 78% in the 3 cases, respectively. The 78% empty structure had the largest forbidden gap in this set and in this paper we will present results on that structure only. We believe 78% is near the optimal volume fraction for this FCC geometry.

Our procedure is similar to the one we used in ref. [8], except that our dynamic range was improved by using an HP-8510 Network Analyzer for all the measurements. The experimental aim is to fully explore all 4π steradians in reciprocal space, while scanning frequency. The valence band edge frequency is defined by a sudden drop in microwave transmission, while the conduction band edge is defined by the frequency at which the transmitted signal recovers. Conservation of wave vector momentum parallel to the slab entry face determines the band edge position along the surface of the Brillouin zone. Since there are two polarizations, we can usually determine the 2 valence band edges and 2 of the conduction bands.

Sometimes the coupling of external plane waves to internal Bloch waves is poor, and the experiment can miss one of the conduction band edges, as happened in ref. [8]. Finite sample size limits the usable dynamic range, exacerbating the weak coupling problem. Therefore, it is important to back up the measurements with numerical calculations, as we have done here. The scalar dielectric constant distribution in fig. 1 is expanded as a Fourier series in the reciprocal space, while Maxwell's equations are expanded [3] as vector plane waves. The eigenvalues converge after a few hundred plane waves are summed in the expansion.

In spite of the non-spherical atoms of fig. 1(b), the Brillouin zone (BZ) is identical to the standard FCC BZ shown in textbooks. Nevertheless, we have chosen an unusual perspective from which to view the Brillouin zone in fig. 3(a). Instead of having the FCC BZ resting on one of its diamond-shaped facets as is usually done, we have chosen in fig. 3(a), to present it resting on a hexagonal face. Since there is a preferred axis for the atoms, the distinctive L-points centered in the top and bottom hexagons are 3-fold symmetry axes, and are labeled L_3. The L-points centered in the other 6 hexagons are symmetric only under a 360° rotation, and are labeled L_1. It is helpful to know that the U_3–K_3 points are equivalent since they are a reciprocal lattice vector apart. Likewise the U_1–K_1 points are equivalent.

Normal incidence on the slab of fig. 2 sends the propagation vector directly toward L_3 in the reciprocal space ("the North pole"). Tilting the angle of incidence moves the propagation vector along a "meridian" toward the "equator". By choosing different azimuthal angles toward which to tilt, the full reciprocal space can be explored. Figure 3(b) shows the dispersion relations along different meridians for our primary experimental sample of normalized hole diameter $d/a = 0.469$ and 78% volume fraction removed. The oval points represent experimental data with s-polarization ($\perp$ to the plane of incidence, $\parallel$ to the slab surface), while the triangular points represent p-polarization ($\parallel$ to the plane of incidence, partially $\perp$ to the slab surface). The horizontal abscissa in the lower graph of fig. 3(b), L_3–K_3–L_1–U_3–X–U_3–L_3 represents a full meridian from the North pole to the South pole of the BZ. Along this meridian the Bloch wave functions separate neatly into s- and p-polarizations. The s- and p-polarized theory curves are the solid and dashed lines, respectively. The dark shaded band is the totally forbidden photonic band gap. The lighter shaded stripes above and below the dark band are forbidden only for s- and p-polarization, respectively.

Along the meridian L_3–W–K_1, the polarizations do not separate neatly, and only the totally forbidden photonic band gap is shaded. The top of the valence band is at W and is mostly s-polarized, but the valence band peaks at U_3, X, and U_1 are almost as high. The bottom of the conduction band is at L_1, purely p-polarized, is only marginally lower than the valley at L_3. We have also measured the imaginary wave vector dispersion within the forbidden gap. At mid-gap we find an attenuation of 10 dB per unit cube length a. Therefore the photonic crystal need not be very many layers thick to effectively expel the zero-point electromagnetic field.

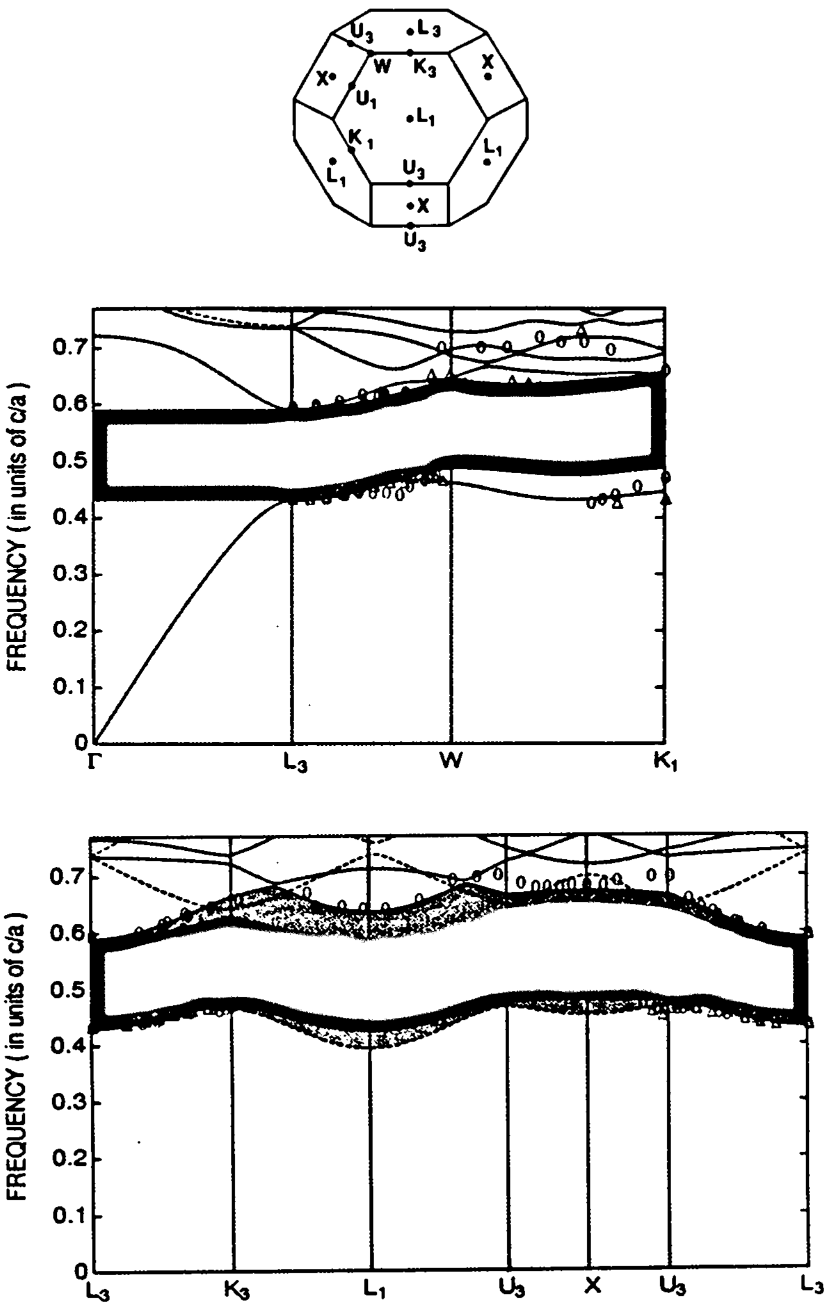

Fig. 3. (a) The Brillouin zone of an FCC structure incorporating non-spherical atoms, as in fig. 1(b). Since the space lattice is not distorted, this is simply the standard FCC Brillouin zone lying on a hexagonal face rather than the usual cubic face. Only the L-points on the top and bottom hexagons are 3-fold symmetry axes. Therefore they are labeled L_3. The L-points on the other 6 hexagons are labeled L_1. The U_3–K_3 points are equivalent since they are a reciprocal lattice vector apart. Likewise the U_1–K_1 points are equivalent. (b) Frequency versus wave vector, ω vs. k, dispersion along the surface of the Brillouin zone shown in 3(a), where c/a is the speed of light divided by the FCC cube length. The ovals and triangles are the experimental points for s- and p-polarization, respectively. The solid and dashed lines are the calculations for s- and p-polarization, respectively. The dark shaded band is the totally forbidden band gap. The lighter shaded stripes above and below the dark band are forbidden only for s- and p-polarization, respectively.

At a typical semiconductor refractive index, $n = 3.6$, the 3-d forbidden gap width is 19% of its center frequency. We have repeated the calculation at lower refractive indices, re-optimizing the hole diameter. Our calculations indicate that the gap remains open for refractive indices as low as $n = 2.1$ using circular holes as in fig. 2. In reactive ion etching, the projection of circular mask openings at 35° leaves oval holes in the material, which might not perform as well. Fortunately we found, defying Murphy's Law, that the forbidden gap width for oval holes is actually improved, fully 21.7% of its center frequency.

In the visible region, there are many transparent optical materials available with a refractive index above 2.1. Furthermore, state-of-the-art reactive ion etching [14] can produce holes that are ≥20 times deeper than their diameter, deep enough to produce an FCC photonic crystal with substantial inhibition in the forbidden gap. It appears that the application of photonic band gaps to semiconductor physics, optical, and atomic physics may soon be practical.

E.Y. would like to thank the authors of ref. [5] for telling about their diamond structure calculations before publication, and for intensive discussions of the degenerate Bloch wave functions at the W-point. John Gural deserves special thanks for this patience, dedication, and skilled machining of tens of thousands of holes, which made this project possible. K.M.L.'s work is supported by ONR contract N00014-88-0500.

References

[1] E. Yablonovitch, Phys. Rev. Lett. 58 (1987) 2059.
[2] S. John, Phys. Rev. Lett. 58 (1987) 2486.
[3] K.M. Leung and Y.F. Liu, Phys. Rev. Lett. 65 (1990) 2646.
[4] Z. Zhang and S. Satpathy, Phys. Rev. Lett. 65 (1990) 2650.
[5] K.M. Ho, C.T. Chan and C.M. Soukoulis, Phys. Rev. Lett. 65 (1990) 3152.
[6] S. John and J. Wang, Phys. Rev. Lett. 64 (1990) 2418.
[7] Y. Yamamoto and S. Machida, Phys. Rev. A 35 (1987) 5114.
[8] E. Yablonovitch, in: Analogies in Optics and Microelectronics, eds. W. van Haeringen and D. Lenstra (Kluwer, Dordrecht, 1990) p. 117.
E. Yablonovitch and T.J. Gmitter, Phys. Rev. Lett. 63 (1989) 1950.
[9] S. Satpathy, Z. Zhang and M.R. Salehpour, Phys. Rev. Lett. 64 (1990) 1239.
[10] K.M. Leung and Y.F. Liu, Phys. Rev. B41 (1990) 10188.
[11] S. John and R. Rangarajan, Phys. Rev. B38 (1988) 10101.
[12] E.N. Economu and A. Zdetsis, Phys. Rev. B40 (1989) 1334.
[13] E. Yablonovitch, unpublished.
[14] A. Scherer, B.P. van der Gaag, E.D. Beebe and P.S.D. Lin, J. Vac. Sci. Technol. B8 (1990) 28.